Special Publication

Characterisation of Porous Solids VIII

Proceedings of the 8th International Symposium on the Characterisation of Porous Solids

Nigel Seaton (Editor), Francisco R Reinoso (Editor), Philip Llewellyn (Editor), Stefan Kaskel (Editor)
ISBN: 978-1-84755-904-3
Copyright: 2009
Format: Hardback
Extent: 464
Price: **£119.95**

BUY PRINT

Author Information

This book is the proceedings of the 8th International Symposium on the Characterisation of Porous Solids that took place in Edinburgh, 10-13th June 2008

SUPERCRITICAL METHANE ADSORPTION – A TOOL FOR CHARACTERIZATION OF CARBONACEOUS ADSORBENTS

M.R. Bałys[1], L. Czepirski[1], S. Furmaniak[2], A.P. Terzyk[2], P.A. Gauden[2]

[1] AGH – University of Science and Technology, Faculty of Fuels and Energy, Department of Coal Chemistry and Adsorption Engineering, al. Mickiewicza 30, 30-59 Cracow, Poland
[2] Nicolaus Copernicus University, Physicochemistry of Carbon Materials Research Group, 7 Gagarin St., 87-100 Toruń, Poland

1 INTRODUCTION

Studies on the physical adsorption of methane on carbonaceous adsorbents at supercritical conditions are stimulated both by theoretical and practical interest. For example, an analytical representation of adsorption equilibrium data is needed in connection with natural gas storage, PSA separation and purification processes, as well as methane recovering from coal seams. Modelling methane isotherms provides an effective tool for studying adsorption mechanism, characterization of porous solids (i.e. pore volume, pore size distribution) and collecting useful information on adsorption systems.[1-10] From a theoretical point of view, this system seems to be interesting, since the intermolecular interactions are relatively simple to modelling for the assumed pore geometry.

In this work high-pressure adsorption isotherms of methane for different carbonaceous adsorbents were analyzed by the potential theory.

Grand Canonical Monte Carlo (GCMC) simulation was also used for calculation of the local adsorption isotherms. The Global Adsorption Isotherm Equation was solved taking the local isotherms (simulated for different pore diameters) as the kernel. Obtained pore size distributions were compared with those calculated from the low – temperature nitrogen adsorption data.

2 EXPERIMENTAL

Two types of carbon materials have been used in this study: a commercial granulated active carbon R2 (Norit, Holland) and monolithic form of active carbon from MAST Carbon Ltd. (Guilford, Great Britain). Porous structure analysis of the samples has been carried out by subatmospheric N_2 adsorption at 77K in a Fisson's Sorptomatic'1900 apparatus.

The measurements of methane adsorption isotherms were made using a modified version of volumetric system described before.[11] The experimental data were measured in the range 276-308K and the pressure range about 0-10 MPa. The pressure was taken by a transducers with the 0,1% accuracy in the whole range. Corrections for the non-ideality of the gas phase were made using the Benedict - Webb - Rubin equation of state. The mean relative uncertainties of the experiments were about 2% by brief error calculations.

3 RESULTS AND DISCUSSION

3.1 Potential theory in interpretation of supercritical adsorption data

Adsorption potential theory, including the Dubinin - Radushkevich (DR) and the Dubinin - Astakhov (DA) equations, has been widely applied to investigating gas adsorption equilibria on microporous adsorbents.[12-14] Although this theory is considered a semiempirical approach, it has achieved great success in many practical applications. The potential theory of adsorption is simply expressed by:

$$W = F(A/\beta) \qquad A = RT\,ln(P_s/p) \tag{1}$$

where: W, F, A and β denote the volume of adsorbed gas, the universal adsorption function, the adsorption potential and the affinity coefficient, respectively. Since there exist a number of ways of representing the saturation vapor pressure, adsorbed volume, and the form of adsorption potential.[15-19]

Methane adsorption isotherms were measured at temperatures above the critical temperature, where the concept of saturation vapor pressure is meaningless. Therefore, above the critical temperatures of adsorbates, one must estimate the ″vapor″ pressures at the adsorption temperatures. This difficulty of correlating data using the potential theory was overcome in the proposed method as follows. First, a hypothetical saturation pressure was calculated using the reduced Kirchhoff equation.

According to Dubinin the purpose of using an affinity coefficient is that all characteristic curves for various adsorbates on a given adsorbent at different temperatures are superimposable on single reduced characteristic curve. In the work, the molar volume of methane in adsorbed state was chosen as this correlating divisor. We propose to introduce so called reduced adsorption potential:

$$A_{red} = A/v^{a} \tag{2}$$

where: v^{β} - the molar volume of methane in adsorbed state. The last one parameter was approximated assuming that gas in adsorbed state can be regarded as a sort of superheated liquid by the method proposed by Ozawa from p-V-T relations reported in literature.[20-21]

Adsorption isotherms of methane at supercritical temperatures and nitrogen at 77K were correlated by plotting the logarithm of the volume adsorbed *vs*. the square of the reduced adsorption potential (Figure 1).

It can be seen that methane characteristic curve is temperature independent and at low values of reduced adsorption potential superimposes on nitrogen characteristic curve. This allows us to conclude that in this region methane adsorption at supercritical temperatures provides similar information as low temperature nitrogen adsorption.

Experimental methane isotherms were also interpreted by the use of the Dubinin - Radushkevich equation. Table 1 contains parameters of microporous structure of active carbons under study obtained from supercritical methane isotherms and low temperature nitrogen isotherms.

The results demonstrate the possibility of application of DR equation for analysis the microporous structure of carbonaceous adsorbents because methane kinetic diameter is enough to be accessible to the micropores of smaller size.

Similar good correlation was also confirmed for experimental data published in literature on supercritical gas adsorption.[22]

Table 1 *Parameters of microporous structure of active carbons calculated from characteristic curve*

	Methane (supercritical)		*Nitrogen (77K)*	
	W_o *[cm* g^{-1}*]*	*E [kJ/mol*$^{-1}$*]*	W_o *[cm* g^{-1}*]*	*E [kJ/mol*$^{-1}$*]*
Norit R2	0.543	9.48	0.539	15.49
Monolith	0.345	11.79	0.337	17.28

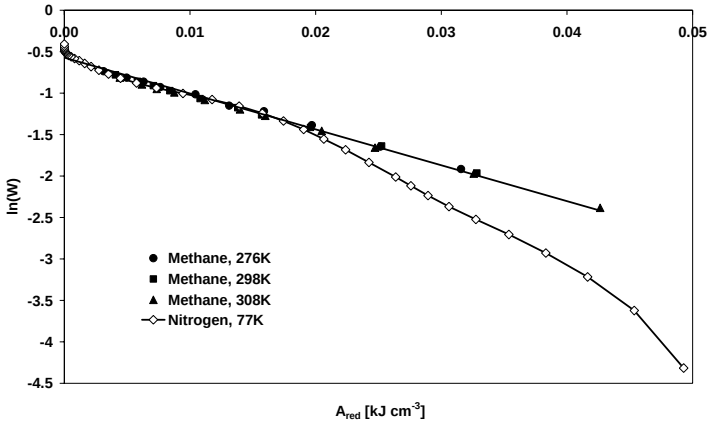

Figure 1 *Generalized characteristic curve for active carbon Norit R2*

The success of this correlation justifies the selection of the molar volume of adsorbed phase as a correlating divisor. Generalized correlation curve was next used for the calculation adsorption equilibrium points for hydrogen on the same carbon at temperatures 196, 243 and 298K. Values of experimental data are compared in Table 2 with those calculated from characteristic curve.

A generalized characteristic curve gives a possibility for succesful prediction of adsorption equilibria for different gases. Only one adsorption isotherm is practically necessary to obtain the characteristic curve and this is sufficient to describe the adsorption at all other temperatures and pressures. The results can be used for the design of adsorption systems and for predicting adsorption equilibrium behaviour of binary and/or multicomponent gaseous mixtures on active carbon under wide range of conditions, without time consuming and expensive experimental determination.

Table 2 *Values of experimental and predicted adsorption for hydrogen on active carbon Norit R2*

T = 196K			*T = 243K*			*T = 298K*		
p	n_{exp}	n_{pred}	*p*	n_{exp}	n_{pred}	*p*	n_{exp}	n_{pred}
MPa	*mmol* g^{-1}		*MPa*	*mmol* g^{-1}		*MPa*	*mmol* g^{-1}	
0.127	0.135	0.137	0.585	0.256	0.248	0.502	0.023	0.026
0.552	1.231	1.228	1.106	0.641	0.629	1.025	0.108	0.113
1.117	2.190	2.187	1.514	1.060	1.048	1.563	0.240	0.244
1.594	2.999	3.009	2.039	1.479	1.488	2.063	0.403	0.410
1.951	3.693	3.702	2.516	1.887	1.902	2.523	0.567	0.571
2.578	4.297	4.288	3.050	2.279	2.268	3.166	0.787	0.792
3.153	4.830	4.815	3.461	2.653	2.641	3.587	0.992	0.996
3.680	5.305	5.330	4.073	3.008	3.020	4.104	1.201	1.210
4.157	5.733	5.740	4.470	3.345	3.336	4.482	1.408	1.395
4.655	6.120	6.115	5.076	3.554	3.544	5.132	1.645	1.652

An important aspect of the design of adsorption process equipment for gas storage and separation is a proper understanding of possible thermal effects. Isosteric heat of adsorption is one of the thermodynamic properties that are of special relevance to gas-phase adsorption systems.

It can be simply expressed analytically from the Clausius - Clapeyron equation and using the DR equation for the equilibrium adsorption isotherm:[23]

$$\Delta H_S = \frac{RT^2}{P_s}\frac{dP_s}{dT} + A - \alpha T\left(\frac{\partial A}{\partial \ln n}\right)_T \qquad n = \frac{W}{v^a} \tag{3}$$

Figure 2 presents the dependence of isosteric heat of methane adsorption on the volume adsorbed for active carbon Norit R2. The run of adsorption heat shows heterogeneity associated with active carbon texture. For the system under study the isosteric heat of adsorption was higher than the heat of condensation and of the sufficient magnitude to be characterized as physical adsorption.

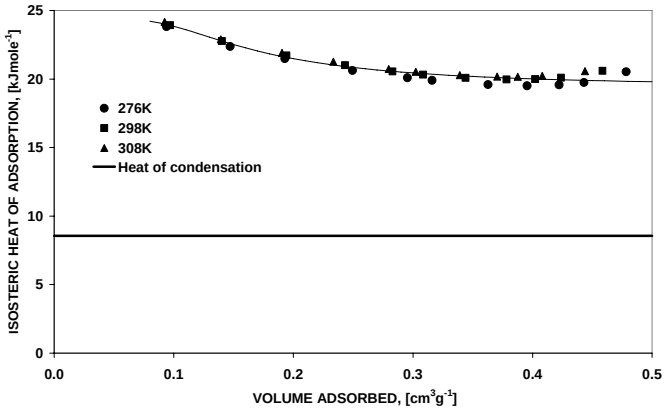

Figure 2 *Isosteric heat of methane adsorption vs. volume adsorbed for active carbon Norit R2*

It was considered that eq. (3) would be sufficient for numerical calculations of thermodynamic characteristics for a given sample as a method facilitating and speeding up calculation for various operative conditions.

3.2 Determination of PSD from low temperature N_2 adsorption data and simulation of methane adsorption in slit-like pores

The PSDs of studied carbons from low temperature nitrogen adsorption isotherms was determined using the method proposed by Nguyen and Do (ND)[24] with the basis of 82 ND local isotherms generated for the same effective width range (from 0.465 to 233.9 nm, i.e. micro-, meso-, and macropores), as in the DFT software (DFT PLUS, ASAP 2010, Micromeritics, USA). The ND method is a relatively simple approach, and leads to exactly the same PSDs as calculated from DFT method (as was shown for many porous materials having different structures and origin - see the results published by Kowalczyk and coworkers.[25] To invert the global adsorption isotherm equation recently proposed *"Karolina"* algorithm was applied.[26]

The Grand Canonical Monte Carlo simulation method of CH_4 adsorption in slit-like pores was applied. For each adsorption point $25 \cdot 10^6$ iterations were performed during the

equilibration, and next $25 \cdot 10^6$ equilibrium ones, applied for the calculation of the averages (one iteration = an attempt to change the state of the system by displacement, creation or annihilation, all three attempts with the same probability).

The energy of fluid-fluid (*ff*) intermolecular interactions between methane molecules was modeled by the five-center potential (each atom is represented by one LJ and electrostatic centre (Table 3), assuming the length of CH bond equal to 0.109 nm):[27]

$$U_{ff}(r) = \sum_{i=1}^{5}\sum_{j=1}^{5}\left[U_{LJ}^{(ij)}(r_{ij}) + U_{C}^{(ij)}(r_{ij})\right] \tag{4}$$

where r is the distance between the mass centers of the interacting molecules, r_{ij} is the distance between the pair of the centers, $U_{LJ}^{(ij)}(r_{ij})$ is the energy of dispersion interactions between the pair of centers modeled using the Lennard – Jones potential:

$$U_{LJ}^{(ij)}(r_{ij}) = \begin{cases} 4\varepsilon^{(ij)}\left[\left(\dfrac{\sigma^{(ij)}}{r_{ij}}\right)^{12} - \left(\dfrac{\sigma^{(ij)}}{r_{ij}}\right)^{6}\right] & r_{ij} < r_{cut}^{(ij)} \\ 0 & r_{ij} \geq r_{cut}^{(ij)} \end{cases} \tag{5}$$

where r_{cut} = 5 σ. The energy of electrostatic interactions between the pair of centers, $U_{C}^{(ij)}(r_{ij})$ was modeled using the approach proposed recently by Fennel and Gezelter[28] (the alternative method to the well-known Ewald summation one):

$$U_{C}^{(ij)}(r_{ij}) = \begin{cases} \dfrac{q_i q_j}{4\pi\varepsilon_0}\left[\dfrac{erfc(\alpha r_{ij})}{r_{ij}} + \dfrac{erfc(\alpha r_{cut,C})}{r_{cut,C}} + \right. \\ \left. + \left(\dfrac{erfc(\alpha r_{cut,C})}{r_{cut,C}^2} + \dfrac{2\alpha\exp(-\alpha^2 r_{ij}^2)}{r_{ij}\sqrt{\pi}}\right)(r_{ij} - r_{cut,C})\right] & r_{ij} \leq r_{cut,C} \\ 0 & r_{ij} > r_{cut,C} \end{cases} \tag{6}$$

where ε_0 is the permittivity of free space (8.8543 $C^2J^{-1}m^{-1}$), and α is the damping parameter. We assumed: α = 2.5 nm^{-1} and $r_{cut,C}$ = 1.5 nm.[28]

The energy of solid-fluid was modeled by the 10-4-3 Steele's potential, where the interaction between methane molecule and carbon wall is given by:

$$U_{sf}(z) = 2\pi\rho\Delta\sum_{i=1}^{5}\varepsilon^{(si)}\left(\sigma^{(si)}\right)^2\left[\frac{2}{5}\left(\frac{\sigma^{(si)}}{z_i}\right)^{10} - \left(\frac{\sigma^{(si)}}{z_i}\right)^{4} - \frac{\left(\sigma^{(si)}\right)^4}{3\Delta\left(z_i + 0.61\Delta\right)^3}\right] \tag{7}$$

where z is a distance between the centre of the mass of CH_4 molecule and carbon wall, z_i is the distance between *i-th* center and the wall, ρ and Δ are the density of carbon atoms forming the wall, and the interlayer spacing (both values were assumed in simulations as the same as for graphite, i.e. ρ = 114 nm^{-3} and Δ = 0.3354 nm).

Table 3 shows the collected values of the applied LJ parameters and the values of charges located on each atom forming methane molecule.

Table 3 *The values of the parameters of LJ potential.[29] The parameters between two different centers were calculated using the Lorentz - Berthelot mixing rules.*

Center	σ [nm]	ε/k_B [K]	q [e]
Fluid			
H	0.281	51.2	+ 0.143
C	0.335	8.6	- 0.572
Solid			
C	0.34	28.0	-

The simulation box was formed from the parallel walls forming a slit-like pore. The following geometric diameters of slits were considered: 0.75, 0.8, 0.85, 0.9, 0.95, 1.0, 1.05, 1.1, 1.15, 1.2, 1.25, 1.3, 1.35, 1.4, 1.5, 1.6, 1.7, 1.8, 1.9, 2.0, 2.1, 2.2 and 2.3 nm (for larger slits no differences between simulated local isotherms were recorded, therefore only micropores are considered). The length of the simulation box was equal to 4 nm, with periodic boundary conditions applied in two remaining directions.

Figure 3 shows examples of simulated methane excess adsorption isotherms in slit-like pores with different geometric diameters.

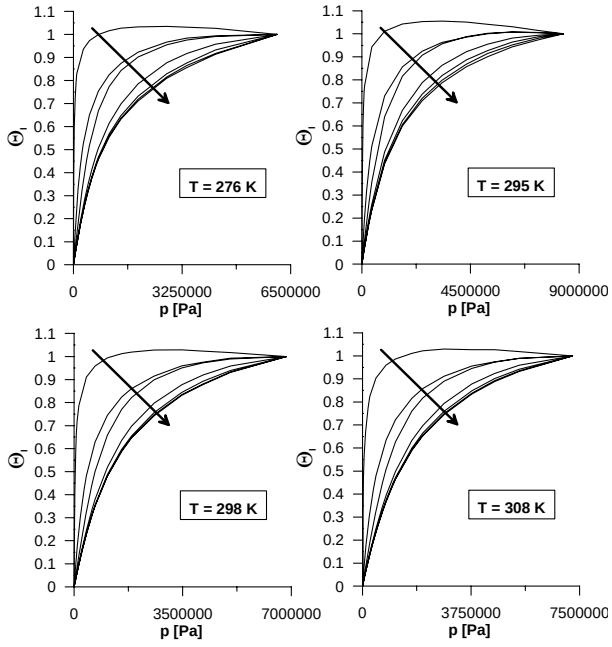

Figure 3 *Examples of simulated excess isotherms of methane adsorption in slit-like pores with geometric diameters: 0.75, 1.0, 1.25, 1.5, 1.8, 2.0, 2.3 nm (the arrow shows the rise in pore diameter).*

One can see that there are not differences recorded between methane adsorption isotherms simulated for pores larger than ca. 2 nm. It is well known fact and therefore one can expect that from methane adsorption data the PSD for larger pores than micropores will not be detected correctly.

Figure 4 shows that for all studied carbons the fit between GCMC results and experimental data is very good however, at larger pressures the deviation occurs. Obtained PSDs from nitrogen adsorption data and ND method show the typical bimodal structure for all studied carbons. This bimodal structure is also recovered from GCMC results of methane adsorption. However in this case, the first peak is usually shifted towards smaller diameters.

The second peak shows the presence of larger pores, and is usually intensive. This shows the weakness of the method. Since there are no remarkable differences observed in local isotherms generated for larger pores than micropores, *"Karolina"* algorithm tries to fit the experimental CH_4 data raising the weights of local isotherms simulated for adsorption in larger pores. Summing up, since all studied carbons contain (sometimes small number) pores larger than micropores the PSD in this range will not be recovered by simulated CH_4 isotherms.

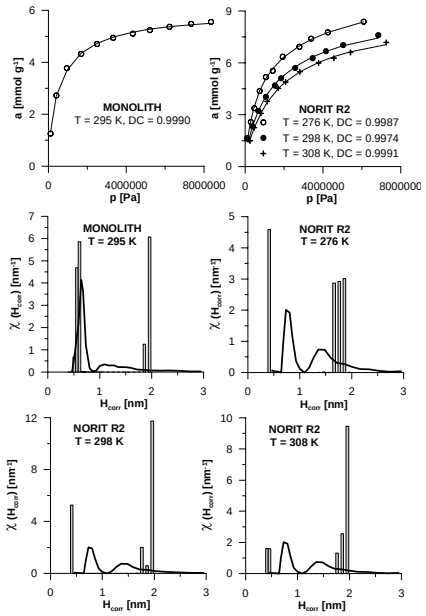

Figure 4 *The results of the fitting of experimental isotherm with "Karolina" algorithm and local isotherms from GCMC simulations. The averaged results from 3 runs are shown (in each run almost the same fit was obtained). Solid line – ND method (nitrogen adsorption at 77 K), bars – methane adsorption.*

The problem in the gap between peaks on PSDs obtained from the set of the local adsorption isotherms (N_2, T = 77K) was previously discussed by Gauden et al.[30] From the comparison of the PSDs collected in Figure 4 one can state that the bimodal shape of distributions is the result of the similarity of adsorption mechanisms and the local adsorption isotherms (for CH_4 more significant than for N_2) in the range of the pore widths for which the gap between peaks (related to the primary and secondary micropore filling mechanism) exists. Therefore, for methane data the first peak on the PSDs is always shifted to smaller pore sizes.

4 CONCLUSIONS

Adsorption potential theory successfully describes the adsorption equilibria of methane on active carbon at supercritical conditions. A generalized characteristic curve gives a possibility for prediction of adsorption equilibria. GCMC simulation was also used for calculation of the local adsorption isotherms and pore size distributions. Both approaches give the possibility to characterize the adsorbent in terms of structural characteristics and obtain the corresponding pore size distributions. In further studies we expect that procedures proposed will be especially useful for characterization of systems with diffusional limitations like carbon molecular sieves or natural coals.

Acknowledgements

The authors from AGH-UST wish to acknowledge to the Ministry of Science and Higher Education for its financial support of this work (PBZ-MEiN-2/2/2006).
The authors from Nicolaus Copernicus University acknowledge the use of the computer cluster at Poznań Supercomputing and Networking Center and the Information and Communication Technology Center of the Nicolaus Copernicus University.

References

1 M.J. Bojan, R. van Sloten, W. Steele, *Separ. Sci. Technol.*, 1992, **27**, 1837.
2 R.F. Cracknell, P. Gordon, K.E. Gubbins, *J.Phys.Chem.*, 1993, **97**, 494.
3 P.B. Balbuena, K.E .Gubbins*, Langmuir*, 1993, **9**, 1801.
4 C.R.C. Jansen, N.A. Seaton*, Langmuir*, 1996, **12**, 2866
5 P.N. Aukett, N. Quirke, S. Riddiford, S.R. Tennison, *Carbon*, 1992, **30**, 913.
6 K. Shethna, S.K. Bhatia, *Langmuir*, 1994, **10**, 870.
7 X.S. Chen, B. Mc Enaney, T.J. Mays, J. Alcaniz - Monge, D. Cazorla - Amoros, A. Linarez-Solano, *Carbon*, 1997, **35**, 1251.
8 J. Jagiełło, P. Sanghani, T.J. Bandosz, J.A. Schwarz, *Carbon*, 1992, **30**, 507.
9 Li Zhou, *Adsorp. Sci. Technol.*, 2005, **23**, 509.
10 Yaping Zhou, Li Zhou, Shupei Bai, Bin Yang, *Adsorp. Sci. Technol.*, 2001, **19**, 681.
11 L. Czepirski, S. Hołda, B. Łaciak, M. Wójcikowski, *Adsorp. Sci. Technol.*, 1996, **14**, 77.
12 D.D. Do, *Adsorption Analysis: Equilibria and Kinetics*, Imperial College Press, London, 1998.
13 R.C. Bansal, M. Goyal, *Activated Carbon Adsorption*, CRC Press, Taylor & Francis Group, Boca Raton FL, 2005.
14 J. Toth, *Adsorption Theory, Modeling and Analysis*, Marcel Decker Inc., New York, 2002.
15 R.K. Agarval and J.A. Schwarz, *Carbon*, 1998, **26**, 873.
16 K.A.G. Amankwah, J.A. Schwarz, 1995, *Carbon*, **33**, 1313.
17 L. Zhan, K.X. Li, R. Zhang, Q.F. Liu, CH.X. Lü, L.Ch. Ling, *J. Supercrit. Fluid*, 2004, **28**, 37.
18 M. Li and A.Z. Gu, *J. Colloid Interf. Sci.*, 2004, **273**, 356.
19 K. Kaneko*, Adsorption*, 1997, **3**, 197.
20 S.Ozawa, S. Kusumi, Y.Ogino, *J. Colloid Interf. Sci.*, 1981, **79**, 399.
21 Li Ming, Gu Anzhong, Lu Xuesheng, Wang Rongshun, *Carbon*, 2003, **41**, 579.
22 L. Szepesy and V. Illes, *Acta Chimica Acad.Sci.Hungaricae*, 1963, **35**, 37.
23 D. Ramirez, Shaoying Qi , M.J. Rood, *Environ. Sci. Technol.*, 2005, **39**, 5864.
24 C. Nguyen and D.D. Do, *Langmuir*, 1999, **15**, 3608.
25 P. Kowalczyk, A.P. Terzyk, P.A. Gauden, R. Leboda, E. Szmechtig-Gauden, G. Rychlicki, Z. Ryu and H. Rong, *Carbon*, 2003, **41**, 1113.
26 S. Furmaniak, A.P. Terzyk, P.A. Gauden, K. Lota, E. Frąckowiak, F. Béguin, P. Kowalczyk, *J. Colloid Interf. Sci.*, 2008, **317**, 442.
27 D.D. Do and H.D. Do, *J. Phys. Chem. B*, 2005, **109**, 19288.
28 Ch.J. Fennel and J.D. Gezelter, *J. Chem. Phys.*, 2006, 234104.
29 S.M. El-Sheikh, K. Barakat, N.M. Salem, *J. Chem. Phys.*, 2006, **124**, 124517.
30 P.A. Gauden, A.P. Terzyk, M. Jaroniec, P. Kowalczyk, *J. Colloid Interf. Sci.*, 2007, **310**, 205.